Comprehensive Analysis and Experiment of Extreme Faults in MMC Based on IGCT

Wenpeng Zhou, *Member, IEEE*, Biao Zhao, *Senior Member, IEEE*, Ruihang Bai, *Member, IEEE*, Yantao Lou, Xiaoping Sun, Qi Liu, Jiapeng Liu, *Student Member, IEEE*, Zhengyu Chen, Jinpeng Wu, Zhanqing Yu, *Member, IEEE*, and Rong Zeng, *Senior Member, IEEE*

***Abstract*—High-voltage direct current voltage source converter (HVdc-VSC) technology is an important solutions for large-scale renewable sources. The MMC is one of the most popular topologies for the HVdc-VSC system. The extreme faults affect the safety and reliability of the MMC greatly. This article gives comprehensive analysis and experiment of extreme faults in the MMC based on an IGCT. Causes and characterization of the extreme faults are analyzed in detail. A new protection solution based on the CP-IGCT and fast recovery diode with HS-FRD is proposed. The surge current capability of HS-FRD is validated via experiment successfully. Theoretical calculation shows that the protection solution based on CP-IGCT, and HS-FRD can help reduce the maximum fault current below 50% when the anode inductor is 0.8 μH in the extreme shoot-through fault. Test results show that the protection solution can realize the discharge of the dc capacitor below 4.5 kV in the extreme shoot-through fault. The maximum fault current in the MMC based on the IGCT is only about 600 kA, while the maximum fault current in the MMC based on the IGBT is over 1100 kA. Explosion proof of CP-IGCT is validated during the tests, which is similar to that of the protection thyristor. However, the IGBT cannot guarantee the stability of the package and may cause severe safety problem. The failed CP-IGCT has the short-circuit failure mode and can be used for bypass of the faulty MMC submodule. Via comparison, the proposed protection solution has lowest cost and complexity, as well as the highest safety.**

***Index Terms*—Explosion proof, extreme fault, fault current, integrated gate commutated thyristor (IGCT), modular multilevel converter (MMC), short-circuit failure mode (SCFM).**

Nomenclature

HVdc-VSC	High-voltage direct current voltage source converter.
MMC	Modular multilevel converter.
IGBT	Insulated gate bipolar transistor.
IGCT	Integrated gate commutated thyristor.
PM-IGBT	Plastic module insulated gate bipolar transistor.
PP-IGBT	Press-pack insulated gate bipolar transistor.
FRD	Fast recovery diode
HS-FRD	Fast recovery diode with high surge current capability
MMC-SM	Modular multilevel converter sub-module
IGCT-SM	MMC-SM based on IGCT.
IGBT-SM	MMC-SM based on IGBT.
CP-IGCT	IGCT with controlled punch-through design.
SCFM	Short-circuit failure mode.

Manuscript received 15 September 2022; revised 5 December 2022; accepted 17 January 2023. Date of publication 1 February 2023; date of current version 10 March 2023. This work was supported in part by National Key R&D Program of China under Grant 2022YFB4200800, and in part by the National Natural Science Foundation of China under Grant 52107156. Recommended for publication by Associate Editor E. Babaei. *(Corresponding author: Rong Zeng.)*

Wenpeng Zhou, Biao Zhao, Ruihang Bai, Jiapeng Liu, Jinpeng Wu, Zhanqing Yu, and Rong Zeng are with the Department of Electrical Engineering, Tsinghua University, Beijing 100084, China (e-mail: 18511829845@163.com; zhaobiao112904829@126.com; bairuihang@qq.com; 18811362403@163.com; wujinpengcn@gmail.com; yzq@tsinghua.edu.cn; zengrong@tsinghua.edu.cn).

Yantao Lou, Xiaoping Sun, and Qi Liu are with the Department of HVDC Technology, Xi'an XD Power Systems Co., Ltd, Xi'an 710065, China (e-mail: louyt@xdps.com.cn; 289817457@qq.com; qliucn@live.cn).

Zhengyu Chen is with the DC Research Center, Sichuan Energy Internet Research Institute, Chengdu 610299, China (e-mail: chenzhen14@tsinghua.org.cn).

Color versions of one or more figures in this article are available at https://doi.org/10.1109/TPEL.2023.3238374.

Digital Object Identifier 10.1109/TPEL.2023.3238374

I. Introduction

THE technology of the HVdc-VSC has developed for many years, and a MMC is one of the most popular topologies for the HVdc-VSC [1], [2]. In the early MMC projects, PM-IGBT are widely applied due to their low costs. However, it is found that PM-IGBTs do not have explosion proof and SCFM [3], [4]. This will bring great risk for the safe operation of the MMC system. Not only the explosion will cause further damage in the surrounding area, the energy of the dc capacitor cannot be discharged due to the open-circuit state of the destroyed device.

Considering this problem, the protection thyristor is usually adopted [5], [6], [7] due to its excellent explosion proof and SCFM. Besides, the protection thyristor is used for sharing the fault current during the dc pole-to-pole short-circuit fault at the same time. This is because the FRD part in PM-IGBT usually has rather a poor surge current capability and cannot withstand the fault current by itself.

With the development of the MMC system with higher voltage and larger capacity, PP-IGBT is preferred in recent years [8], [9], [10]. This is because PP-IGBTs have higher blocking voltage and larger working current compared with PM-IGBTs. Meanwhile, the dc capacitor in MMC based on PM-IGBTs has a larger capacitance and a higher rated voltage. This means that the dc capacitor stores larger energy and discharge of such large energy is more important when an overvoltage fault event happens. Following the old design, the protection thyristor with higher voltage and larger capacity can be applied. However, the extra protection thyristor with such power level will increase the complexity and cost of the

MMC system greatly. As a result, there is urgent need for the alternative protection solutions for the protection thyristor.

With the development of FRD's manufacture technology, a kind of HS-FRD can withstand the fault current in the dc pole-to-pole short-circuit fault by itself [11]. As a result, the protection thyristor can be saved in the MMC system. However, there still needs a way for limiting the overvoltage of the dc capacitor and dealing with the extreme shoot-through fault. The only possible way is to let the main switch get destroyed under a certain overvoltage and let the capacitor's energy discharged, which is just like the protection thyristor.

The IGCT is another kind of press-pack high power device. It has lower voltage drop, smaller manufacture cost, and lower failure rate than PP-IGBT [12], [13], [14], [15]. Besides, a new developed CP-IGCT has been developed [16]. And it can be used for limiting the overvoltage of dc capacitor and discharge the stored energy. Though the operation characteristics of the MMC based on the IGCT has been discussed a lot [17], [18], [19], [20], there is no relative discuss on the analysis and experiment of extreme faults in MMC based on the IGCT.

This article gives comprehensive analysis and experiment of extreme faults in MMC based on the IGCT. Section II analyzes the causes and characterization of extreme faults in the MMC system. Section III proposes the new protection solution for the extreme faults in MMC based on the IGCT. Section IV analyzes the characterization of the extreme shoot-through fault current in the MMC based on the IGCT. Section V gives the system-level experiment validation of the proposed protection solution for the extreme faults in the MMC based on the IGCT. Section VI gives comprehensive comparison of different protection solutions in MMC system on the safety, cost, and complexity. Finally, Section VII concludes this article.

II. Causes and Characterization of Extreme Faults in the MMC System

A. Extreme Shoot-Through Fault in the MMC system.

The shoot-through fault is one of the common severe faults in the MMC system [21]. For the typical MMC based on 4.5-kV high power devices, the dc capacitor in the MMC system is usually above 10 mF with the rated voltage of more than 2 kV. As a result, the dc capacitor stores much energy. When the dc capacitor discharges through the small inductance in the MMC-SM due to unexpected device failure or system fault, the devices in the MMC-SM will suffer a huge surge current. And stable explosion-proof and SCFM of the failed devices can guarantee the safe operation of the MMC system.

However, the shoot-through fault of MMC-SM does not always happen under the rated voltage and an extreme one under the overvoltage condition may occur. Fig. 1 illustrates this kind of extreme shoot-through fault. Fig. 1(a) gives the topology of the MMC system, and Fig. 1(b) shows the shoot-through path in the MMC-SM.

When S_1 and K totally lose control (the MMC-SM becomes "black") due to the controller or communication faults, the capacitor's energy cannot be discharged through S_1. To reduce the effects of this fault event on power transmission reliability and

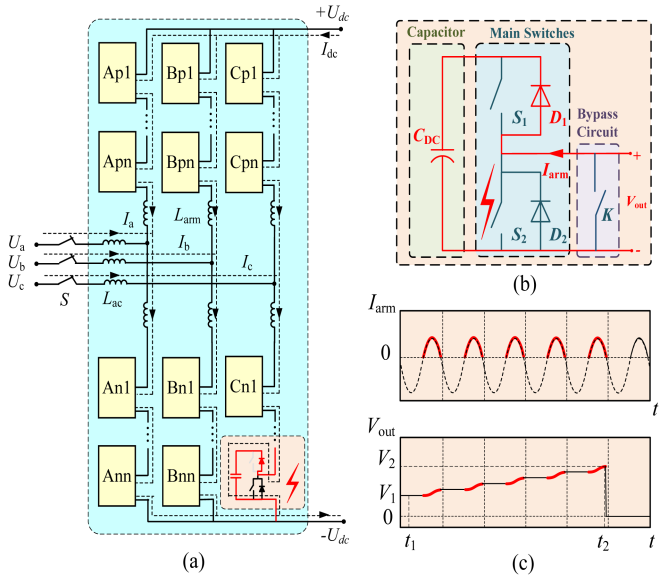

Fig. 1. Illustration of the extreme shoot-through fault in the MMC system. (a) Topology of the MMC system. (b) Shoot-through path in the MMC-SM. (c) Illustration of the arm current and the output voltage waveform of the faulty MMC-SM.

maintenance cost, the whole MMC system should try to avoid stopping. Then, in this situation, the capacitor's voltage will be charged to a much higher value than the rated voltage via D_1 by the arm current I_{arm}, as shown in Fig. 1(c). During the charging period, S_2 and D_2 both suffer the capacitor's overvoltage until one of them is destroyed under the overvoltage, which is higher than the breakdown voltage (for example, the breakdown voltage of 4.5-kV devices is usually higher than 4.5 kV). After that, the dc voltage will transfer to the upper devices gradually. And this means that D_1 will get into the reverse recovery period. This reverse recovery process under such high overvoltage is far beyond D_1's safe operation area and it will get destroyed, too. Because both the upper and lower devices cannot withstand the capacitor's dc voltage, a discharging loop of the capacitor's energy will be formed by them and the extreme shoot-through fault happens.

However, the breakdown voltage of power devices are not constant and the device damage may happen under a much higher overvoltage than its rated blocking voltage. As a result, there may be much electrical and thermal stress on the capacitor. This will bring large challenge for the safe operation of the MMC system due to the risk of capacitor's destruction and explosion. As a result, there needs a way to discharge the capacitor's energy and limit the continuous increase of the capacitor's voltage.

B. DC Pole-to-Pole Short-Circuit Fault in the MMC System

Another extreme fault in the MMC system is the dc pole-to-pole short-circuit fault. When this fault happens, the MMC system works in the uncontrolled rectification state due to the blocking of all the main switches. This means that the lower diode D_2 in every MMC-SM needs to withstand the short current before the ac circuit breaker S works, as shown in Fig. 2. The delay time of the ac circuit breaker's action is usually about

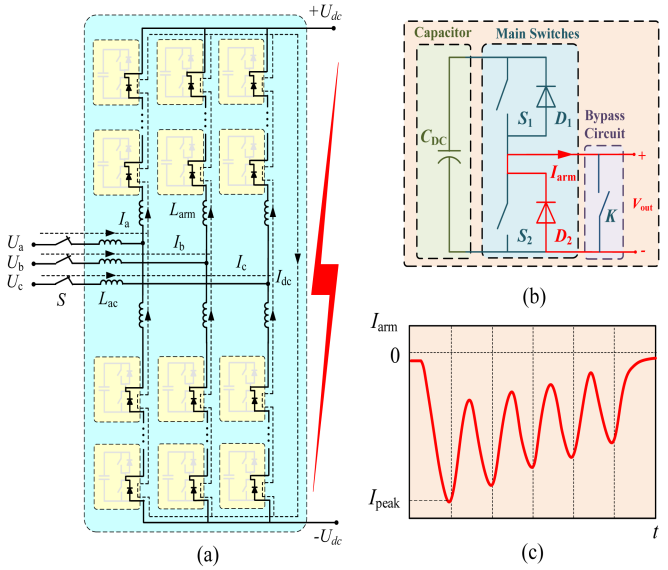

Fig. 2. Illustration of the DC pole-to-pole short-circuit fault in the MMC system. (a) Topology of the MMC system. (b) Short-circuit current path in MMC-SM. (c) Illustration of the short-circuit current waveform in the MMC system.

100 ms after the fault happens. As a result, the lower diode D_2 needs to suffer a continuous surge current for about 100 ms. If the surge current capability of the lower diode is poor, all the lower diodes may get destroyed during this fault. As a result, there needs a way to help the lower diodes get through the surge current during this fault.

III. Proposed Solution for Overcoming Extreme Faults in MMC Based on IGCT

A. Protection Solutions in MMC Based on the IGBT

In MMC based on the IGBT, the integrated diodes in IGBTs usually cannot withstand the fault current in the dc pole-to-pole short-circuit fault. As a result, the protection thyristor is applied for sharing the fault current and protecting the diodes, as shown in Fig. 3(a). In addition, the breakdown voltage of the protection thyristor (reverse voltage) is designed for a constant value. As a result, the protection thyristor can also limit the overvoltage of the dc capacitor and let the capacitor's energy run through the destroyed thyristor.

With the development of diode's manufacture technology, HS-FRD can withstand the fault current in the dc pole-to-pole short-circuit fault by itself. As a result, the protection thyristor can be saved in the MMC system. However, there still needs a way for limiting the overvoltage of the dc capacitor and dealing with the extreme shoot-through fault. Here, the active-clamp circuit of the IGBT can be used.

The active-clamp circuit in the IGBT is usually used for limiting the overvoltage during IGBT's turn-OFF process [22], [23], [24], [25]. In addition, it is also applied for overvoltage protection of the IGBT [26], [27]. The basic principle of the active-clamp circuit in the IGBT is illustrated in Fig. 3(b). When the overvoltage of the IGBT is higher than the designed value, the transient-voltage suppression (TVS) diode D_3 breaks down and the capacitor between the gate and emitter of the IGBT is charged up with the avalanche current of D_3. The quasi-equilibrium voltage applied to the gate of the IGBT is affected by the applied reverse voltage V_{off2} and gate resistance R_{g2}. If the gate–emitter of the IGBT is forward biased, the collector voltage will fall with the rising of the collector current.

When the MMC-SM gets blocked, the IGBT will suffer from the overvoltage and the collector current for a rather long time under the effect of the active-clamp circuit. The accumulated heat in the device will get it destroyed thermally. Then, the capacitor's energy will run through the destroyed IGBT. As a result, the overvoltage of the dc capacitor can be limited.

B. Proposed Solution in MMC Based on the IGCT

The proposed solution in the MMC based on the IGCT is illustrated in Fig. 3(c). Similar to the protection solution based on the IGBT with the active-clamp circuit, HS-FRDs are also applied for dealing with the dc pole-to-pole short-circuit fault. To limit the overvoltage of the dc capacitor and deal with the extreme shoot-through fault, the CP-IGCT can be applied [16].

The principle of the CP-IGCT is to arrange a weak voltage point in the center of the chip through controllable punch-through design, which is similar to the design in the protection thyristor [5], [6]. However, the principle of CP-IGCT's breakdown is not based on avalanche multiplication. So, the breakdown voltage is slightly dependent on temperature and the voltage discrepancy is small under different operation temperatures.

In Fig. 3, it can be seen that the proposed solution based on CP-IGCT and HS-FRD in MMC based on the IGCT does not need the extra protection thyristor or the active-clamp circuit in gate drive. As a result, this solution can reduce the complexity and cost greatly [16].

IV. Characterization of the Extreme Shoot-Through Fault Current in the MMC Based on the IGCT

A. Stray Inductance Analysis in Different MMC-SMs

The equivalent circuits of IGCT-SM and IGBT-SM are compared in Figs. 4 and 5. Due to the differences of turn-ON characteristics between IGBT and IGCT, a di/dt limiting inductor (L_{A}) is needed in IGCT-SM. Besides, a clamp circuit is also needed to limit IGCT's turn-OFF overvoltage caused by L_{A}, including the diode D_{CL}, the resistor R_{CL}, and the capacitor C_{CL}.

When the extreme shoot-through fault happens, the energy of the dc capacitor runs through the main switches, as well as the heat sinks and the copper bars for connection. The total inductance along the discharging loop affects the peak fault current significantly. The stray inductance distribution in IGCT-SM and IGBT-SM are shown in Figs. 4 and 5 respectively. Compared with IGBT-SM, the stray inductance in IGCT-SM has been designed carefully to avoid severe current oscillation during the operation [11].

Then, the stray inductances in IGCT-SM and IGBT-SM are extracted in Ansys Q3d based on the 3-D structures of different MMC-SMs. The extracted results of IGCT-SM show that the

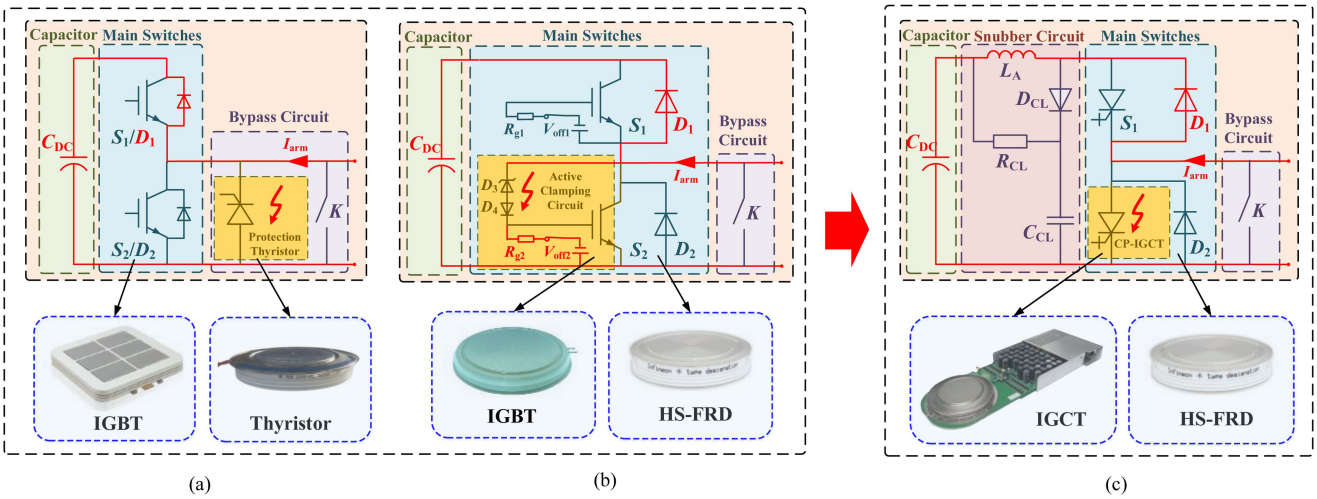

Fig. 3. Comparison of different protection solutions for handling with the extreme shoot-through fault and DC pole-to-pole short-circuit fault in the MMC system. (a) Protection solution using the protection thyristor in the MMC based on the IGBT. (b) Protection solution using the IGBT with the active-clamp circuit and HS-FRD. (c) Protection solution using CP-IGCT and HS-FRD.

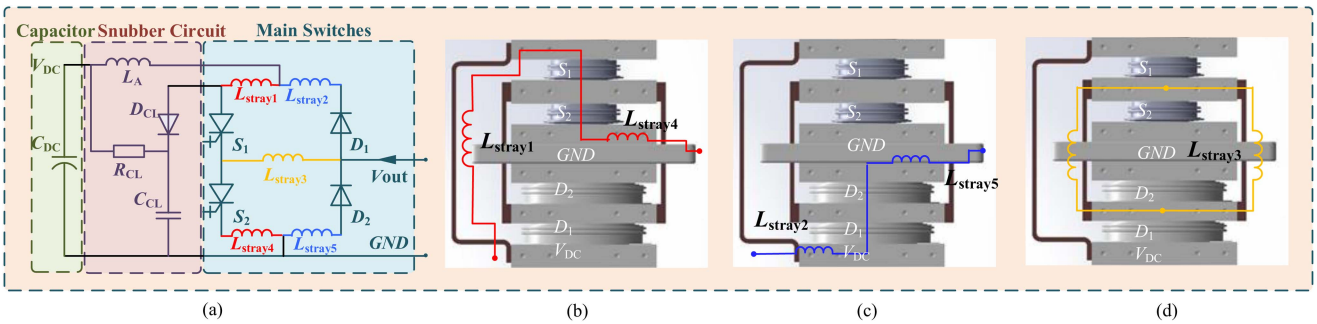

Fig. 4. Equivalent circuit of IGCT-SM based on the practical structure. (a) Equivalent circuit including the stray inductances. (b) Positions of $L_{\mathrm{stray}1}$ and $L_{\mathrm{stray}4}$. (c) Positions of $L_{\mathrm{stray}2}$ and $L_{\mathrm{stray}5}$. (d) Positions of $L_{\mathrm{stray}3}$.

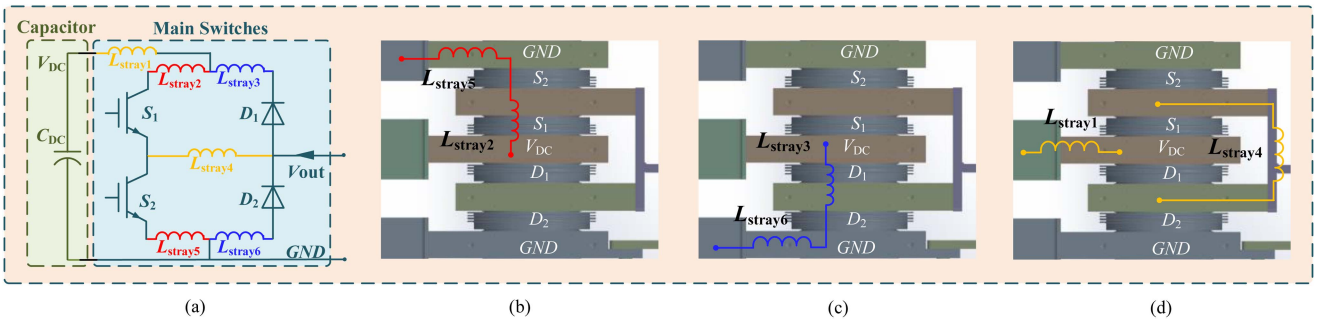

Fig. 5. Equivalent circuit of IGBT-SM based on the practical structure. (a) Equivalent circuit including the stray inductances. (b) Positions of $L_{\mathrm{stray}2}$ and $L_{\mathrm{stray}5}$. (c) Positions of $L_{\mathrm{stray}3}$ and $L_{\mathrm{stray}6}$. (d) Positions of $L_{\mathrm{stray}1}$ and $L_{\mathrm{stray}4}$.

total inductance of the discharging loop is near 1 μH including L_{A}, $L_{\mathrm{stray}2}$, $L_{\mathrm{stray}3}$, and $L_{\mathrm{stray}4}$. While the extracted results of IGBT-SM show that the total inductance of the discharging loop in IGBT-SM is below 0.2 μH including $L_{\mathrm{stray}1}$, $L_{\mathrm{stray}3}$, $L_{\mathrm{stray}4}$, and $L_{\mathrm{stray}5}$. This indicates that a larger fault current will appear in IGBT-SM under the same circuit condition.

B. Fault Current Calculation in Different MMC-SMs

Take the conducting path formed by failed D_1 and S_2 in the MMC-SM, for example, the fault current i_{f} during the extreme shoot-through fault flows through the MCC submodule and can be analytically expressed as follows (by solving the differential

TABLE I
COMPARISON OF BASIC CIRCUIT PARAMETERS OF IGBT-SM AND IGCT-SM DURING THE EXTREME SHOOT-THROUGH FAULT

MMC-SM	IGBT-SM	IGCT-SM
C_{DC}	12-18 mF	12-18 mF
V_C	4.5 kV	4.5 kV
L_A	No need	Needed
L_s	0.14 μH	0.13 μH
$R_{d,\ diode}$	0.30 mΩ	0.30 mΩ
$R_{d,\ IGCT/IGBT}$	0.41 mΩ	0.28 mΩ

equation in the second-order *R-L-C* system under the under-damped process):

$$i_f(t) = V_C/(L\omega_o) \cdot \exp(-t/\tau) \cdot \sin(\omega_o t) \tag{1}$$

where V_C is the voltage of the dc capacitor. ω_o, L, R, and τ are given from (2) to (5) as follows. L_s and R_s represent the stray inductance and resistance along the conducting path. ESR represents the resistance in the dc capacitor. R_d represents the resistance of the devices. Because R_s and ESR are usually much smaller than R_d, R can be approximately estimated as R_d.

$$\omega_o = \sqrt{1/LC - R^2/4L^2} \tag{2}$$

$$L = L_A + L_s \tag{3}$$

$$R = R_d + \mathrm{ESR} + R_s \approx R_d \tag{4}$$

$$\tau = 2L/R. \tag{5}$$

Then, the peak value $i_{f,\ max}$ of the fault current and the time instant $t_{f,\ max}$ can be calculated as follows:

$$i_{f,max} = V_C/L\omega_o \cdot \exp[-\arctan(\omega_o\tau)/\omega_o\tau] \cdot \sin[\arctan(\omega_o\tau)] \tag{6}$$

$$t_{f,max} = \arctan(\omega_o\tau)/\omega_o. \tag{7}$$

Table I gives the basic circuit parameters of IGCT-SM and IGBT-SM. The capacitance is 12–18 mF and the voltage during the extreme shoot-through fault is set 4.5 kV. The total stray inductances along the discharging loop are extracted in Section IV-A. Resistances of the devices are obtained from the datasheets [28], [29], [30], which ignore temperature dependencies, resistances of the packaging, and the knee voltage during *I–V* curves [31].

To illustrate anode inductor's limitation on the fault current in IGCT-SM, $i_{f,max}$–L_A curves in IGCT-SM and IGBT-SM are plotted in Fig. 6. Three kinds of capacitance conditions are compared. Take the fault current in IGBT-SM as the reference (points where the assumed L_A is 0.01 μH in Fig. 6, normalized fault currents in IGCT-SM are listed in Table II. According to the results, the fault current in IGCT-SM is about 55%, 43%, and 36% that in IGBT-SM when L_A is 0.4, 0.8, and 1.2 μH, respectively. And the results are almost the same under different capacitance conditions.

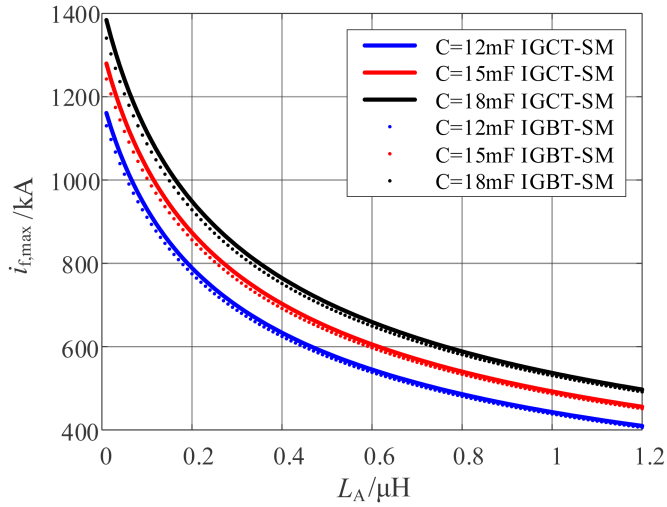

Fig. 6. $i_{f,max}$–L_A curves in IGCT-SM and IGBT-SM under different DC capacitances during the extreme shoot-through fault.

TABLE II
QUANTITATIVE COMPARISON OF FAULT CURRENTS IN IGBT-SM AND IGCT-SM DURING THE EXTREME SHOOT-THROUGH FAULT

MMC-SM	IGBT-SM	IGCT-SM		
	0.01 μH	0.4 μH	0.8 μH	1.2 μH
12 mF	100%	55%	43%	36%
15 mF	100%	56%	43%	36%
18 mF	100%	56%	43%	37%

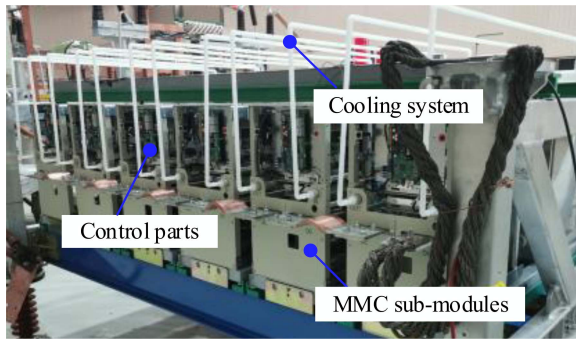

Fig. 7. Picture of the built the experiment platform including two MMC bridges with 12 MMC-SMs for validating the extreme shoot-through fault and DC pole-to-pole short-circuit fault.

V. EXPERIMENT VALIDATION OF THE PROPOSED PROTECTION SOLUTION IN MMC BASED ON IGCT

A. System-Level Experimental Platform

To validate the proposed protection solution for extreme faults in the MMC based on IGCT, an experiment platform based on two MMC bridges is built. The single MMC bridge is shown in Fig. 7. The MMC bridge consists of six MMC-SMs, as well as the cooling system and control parts.

Fig. 8 gives the topologies for validating the extreme faults in the MMC system. The transformer *T* supplies the voltage of

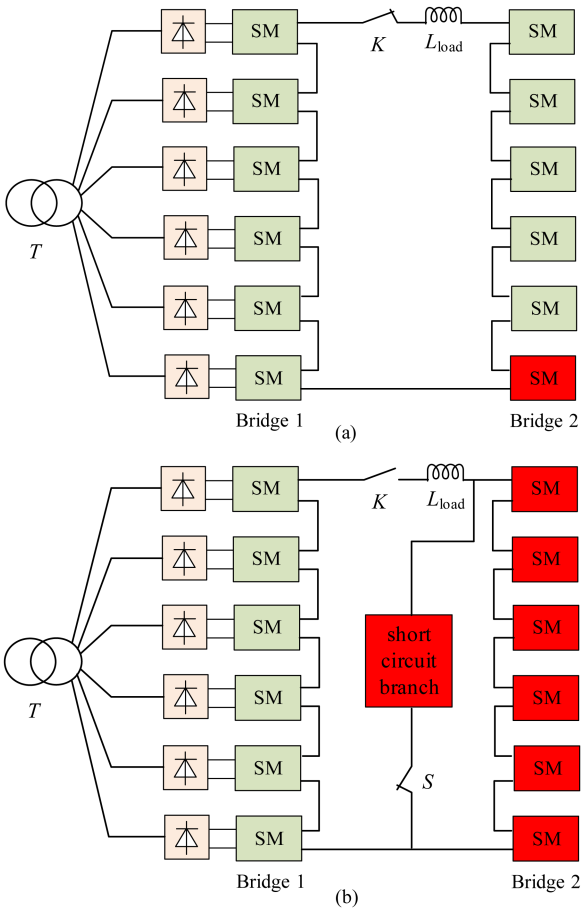

Fig. 8. Topologies for validating the extreme faults in the MMC system. (a) Topology for validating the extreme shoot-through fault. (b) Topology for validating the DC pole-to-pole short-circuit fault.

two MMC bridges through the diode rectifier bridge. $L_{\rm load}$ is connected between two MMC bridges to help control the load current. The circuit breaker *K* is used to cut off the fault current when the overcurrent fault occurs.

When the extreme shoot-through fault is tested, the system is first put into operation for certain time until the devices go into thermal stability. Then, one of the MMC-SMs is forced into blocking state and the load current charges the dc capacitor in the blocked MMC-SM to increase the dc capacitor's voltage, as shown in Fig. 8(a). When the voltage achieves the breakdown voltage of the lower main switch or the protection thyristor in the MMC-SM, the extreme shoot-through fault happens. Then, the destroyed device will bypass the faulty MMC-SM.

When the dc pole-to-pole short-circuit fault is tested, the system is also put into operation for certain time until the devices go into thermal stability firstly. Then, the two bridges are disconnected by cutting off *K* and a short-circuit branch is connected to the bridge under test by *S* to generate the dc pole-to-pole short-circuit current, as shown in Fig. 8(b).

B. Experiment Validation of DC Pole-to-Pole Short-Circuit Fault

The test result of the dc pole-to-pole short-circuit fault in the MMC system is shown in Fig. 9. The tested bridge is

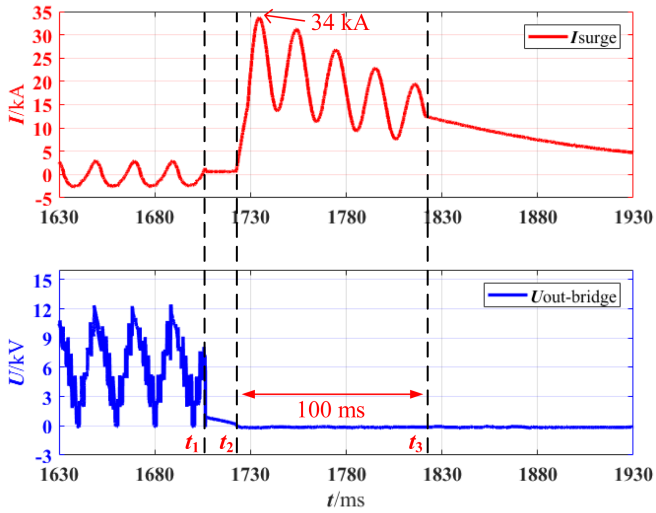

Fig. 9. Test results of the surge current and bridge output voltage test result during the DC pole-to-pole short-circuit fault in the MMC system.

disconnected with the other bridge at t_1 and the short-circuit branch is connected with the tested bridge at t_2 to start the dc pole-to-pole short-circuit fault. Then, the fault is stopped at t_3 after about 100 ms, which simulates the action delay of the ac circuit breaker in the real MMC system.

The tested surge current lasts for about 100 ms with five working cycles. The peak current of the surge current is about 34 kA. When using the protection thyristor, the function of its current sharing can help all the diodes get through this fault current. While when using HS-FRDs, the junction temperature of HS-FRD can be controlled in the safe range due to its larger chip area and lower thermal resistance. And the characteristics of all HS-FRDs keeps well after the test and this verifies the excellent surge current capability of HS-FRDs.

C. Experiment Validation of the Extreme Shoot-Through Fault

The test result of the extreme shoot-through fault in the MMC system is shown in Fig. 10. The output voltage of the MMC-SM durng the normal operation is about 2.2 kV. When the tested submodule is blocked at t_4, the capacitor voltage in the blocked submodule is charged to about 4.5 kV after about 150 ms. Then, the output voltage of the blocked submodule suddenly falls at t_5, which means that the extreme shoot-through fault happens at this time.

Figs. 11–13 give the tested results of the fault current and the output voltage of MMC-SMs based on different protection solutions. For the protection solution based on CP-IGCT and HS-FRD, the peak value of the fault current is about 600 kA. And the output voltage decreases quickly within 1 μs when it achieves the breakdown voltage of CP-IGCT, which is about 4.5 kV.

For the protection solution based on the protection thyristor, the extreme shoot-through fault happens at about 4.2 kV and the output voltage of MMC-SM also decreases quickly in several microseconds. However, due to the low total stray inductance along the discharging loop in the submodule, the peak value of the fault current is about 1000 kA.

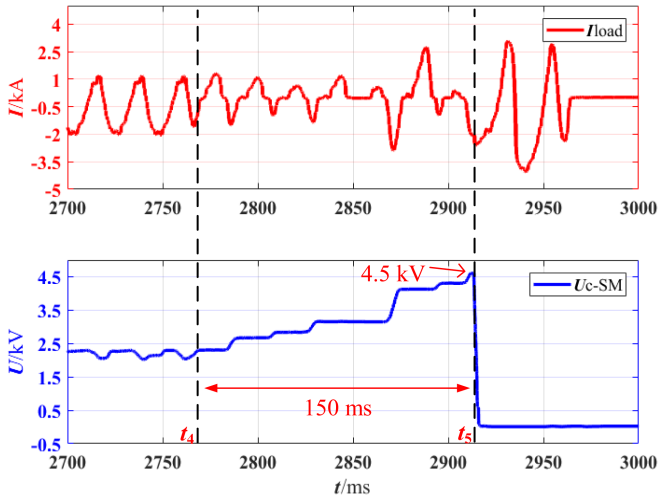

Fig. 10. Test results of the load current and MMC-SM's output voltage during the extreme shoot-through fault in the MMC system.

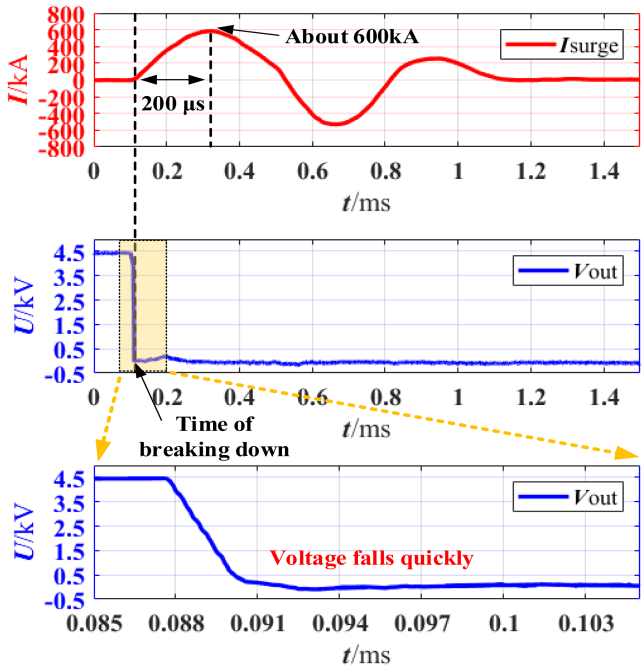

Fig. 11. Test results of the blocked IGCT-SM's fault current and output voltage during the extreme shoot-through fault in the MMC system.

While for the protection solution based on the IGBT with the active-clamp circuit and HS-FRD, the extreme shoot- through fault happens at around 4.5 kV. The output voltage of the MMC-SM decreases to a low value after about 85 μs. Similarly, the peak value of fault current is over 1100 kA due to the low total stray inductance along the discharging loop.

The tested fault currents in different protection solutions prove the accuracy of the current estimation in Section IV. The limitation of the anode inductor on the fault current in the MMC based on the IGCT is validated.

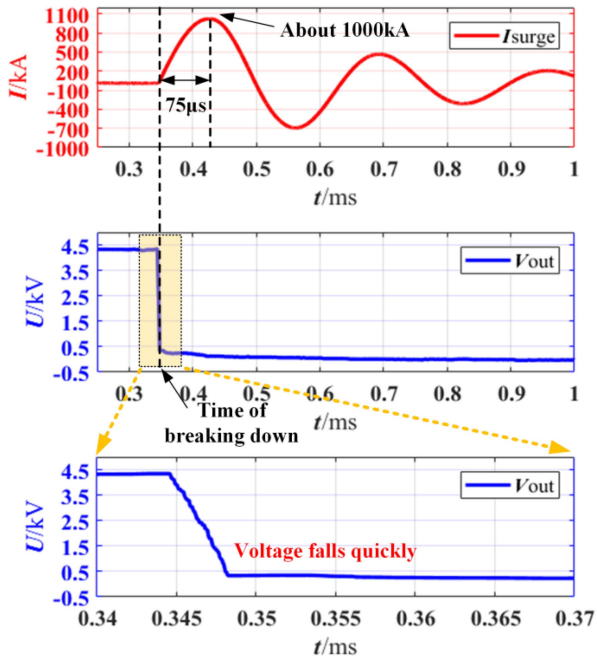

Fig. 12. Test results of the blocked IGBT-SM's fault current and output voltage using the protection thyristor during the extreme shoot-through fault in the MMC system.

VI. Comprehensive Comparison of Different Protection Solutions on Safety, Cost, and Complexity

A. Safety Comparison of Different Protection Solutions

Fig. 14 gives the comparison of the housing packages and inner chips after the extreme shoot-through faults using different protection solutions. Fig. 14(a) gives the picture of destroyed CP-IGCT, while Fig. 14(b) and (c) give pictures of the destroyed thyristor and IGBT, respectively.

It can be seen that housing packages of destroyed CP-IGCT and the protection thyristor maintain well without any crack. This validates excellent explosion proof of the IGCT and the protection thyristor. Comparing the inner chips, it can be seen that the central areas are destroyed severely. This means that the capacitor's energy is mainly focused in the chip center, as shown in Fig. 15(a). As a result, the produced heat can be evenly transmitted inside the housing package and the thermal stress of the ceramic shell is reduced greatly [32].

While the housing package of destroyed IGBT gets cracked severely. This can be explained as follow. The high-power IGBT is formed with tens of paralleled IGBT chips, as shown in Fig. 15(b). The characteristic differences among these chips make the destroyed positions under such a large fault current also random. When the active-clamp circuit works, the chip located at the package edge may get destroyed first, and then, the huge energy may focus here and cause the package to suffer great thermal stress.

Besides, it can be found that the failed IGBT cannot get into the low-resistance state quickly. According to the magnified output voltage waveform in Fig. 13, the destroyed IGBT

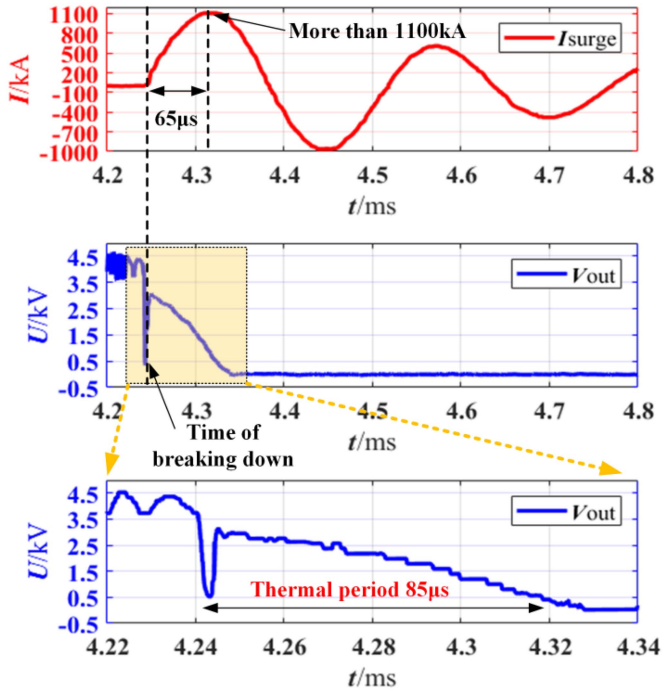

Fig. 13. Test results of the blocked IGBT-SM's fault current and output voltage using the IGBT with the active-clamp circuit during the extreme shoot-through fault in the MMC system.

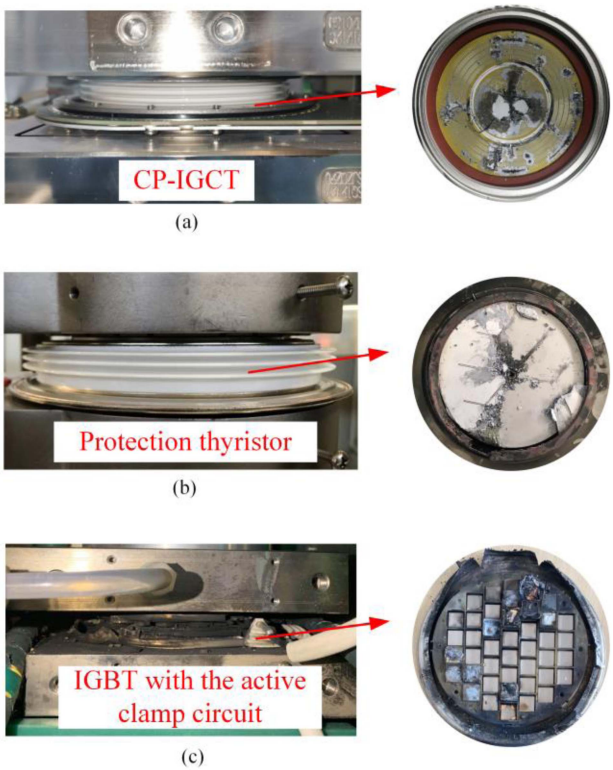

Fig. 14. Comparison of the housing packages and inner chips after the extreme shoot-through faults. (a) Housing package and the inner chip of CP-IGCT. (b) Housing package and the inner chip of the protection thyristor. (c) Housing package and inner chips of IGBT with the active-clamp circuit.

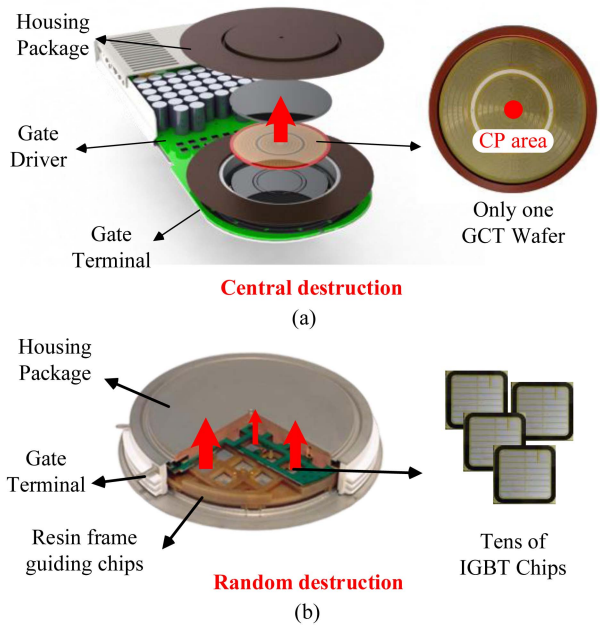

Fig. 15. Comparison of the destruction positions of CP-IGCT and IGBT with the active-clamp circuit. (a) Central destruction of CP-IGCT, which is similar to that of the protection thyristor. (b) Random destruction positions of IGBT with the active-clamp circuit.

experiences a thermal period of about 85 μs with both high current and high voltage. And there is no such phenomenon in destroyed CP-IGCT or protection thyristor. As a result, the destroyed IGBT suffers much higher heat than CP-IGCT and protection thyristor during this period. This will increase the transient temperature inside the packaging and cause great thermal stress of the ceramic shell. As a result, the explosion proof of the failed IGBT with the active-clamp circuit cannot be guaranteed.

Fig. 16 gives SCFM comparison of the destroyed IGCT, protection thyristor, and IGBT with the active-clamp circuit. All devices are tested under the 3000-A dc current for more than 12 h continously. The monitored voltage drops show that all the destroyed devices are suitable for bypassing the faulty MMC-SMs. The destroyed IGCT has a quite low voltage drop with an average short resistance below 0.15 mΩ. The destroyed protection thyristor and IGBT have average short resistances of about 0.33 and 0.27 mΩ, respectively. The formed silicon-aluminum alloy area in the failed devices contributes to the stable SCFM [33]. Safety comparison of different protection solutions for handling with extreme faults is given in Table III.

B. Cost and Complexity Comparison of Different Protection Solutions

Cost comparison of different protection solutions is illustrated in Table IV. There is no need for the extra gate drive circuits and protection thyristor in IGCT-SM, compared with IGBT-SM. However, the clamp circuit is necessary and the power supply module is more expensive for larger power requirements. In

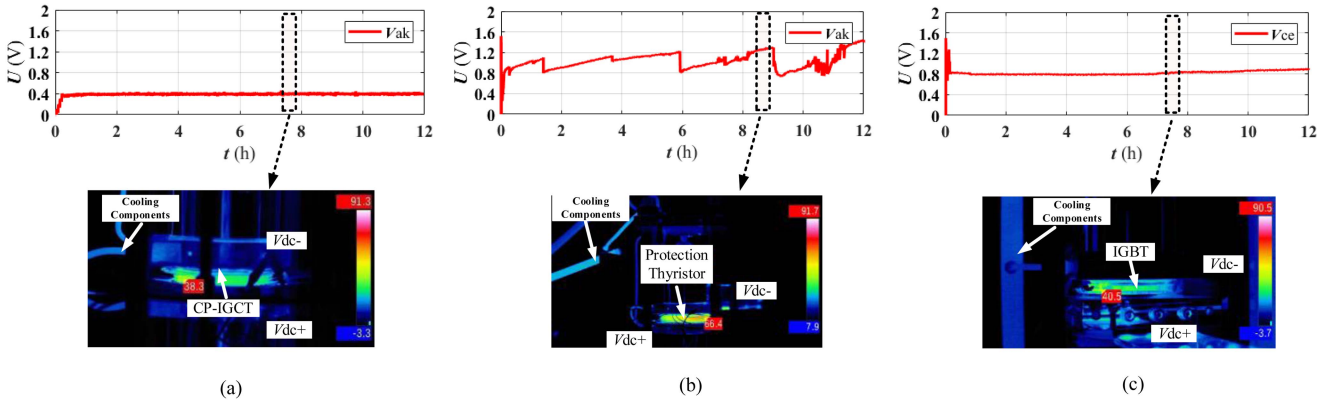

Fig. 16. SCFM comparison of the destroyed IGCT, protection thyristor and IGBT with the active-clamp circuit during the long term short-circuit tests under 3000-A DC. (a) Monitored voltage drop and temperature of the destroyed IGCT in IGCT-SM. (b) Monitored voltage drop and the temperature of the destroyed protection thyristor in IGBT-SM. (c) Monitored voltage drop and the temperature of the destroyed IGBT in IGBT-SM.

TABLE III
SAFETY COMPARISON OF DIFFERENT PROTECTION SOLUTIONS BASED ON CP-IGCT, IGBT WITH ACTIVE-CLAMP CIRCUIT, AND PROTECTION THYRISTOR

Scheme	CP-IGCT	IGBT with active clamp circuit	Protection thyristor
Fault current	1000 kA	1100 kA	600 kA
Destroyed areas	Near center	Random	Near center
Explosion proof	Yes	No	Yes
SCFM	Yes	Yes	Yes

TABLE IV
COST COMPARISON OF DIFFERENT PROTECTION SOLUTIONS BASED ON CP-IGCT, IGBT WITH ACTIVE-CLAMP CIRCUIT, AND PROTECTION THYRISTOR

Scheme	CP-IGCT	IGBT with active clamp circuit	Protection thyristor
Main switches	3.4 p.u.	4.8 p.u.	6.0 p.u.
Discrete diodes	0.4 p.u.	0.4 p.u	/
Protection thyrsitor	/	/	0.8 p.u.
Gate drive unit	/	0.8 p.u.	0.6 p.u.
Power supply module	0.6 p.u.	0.2 p.u.	0.2 p.u.
Clamp circuit	0.2 p.u.	/	/
Total cost	4.6 p.u.	6.2 p.u.	7.6 p.u.

general, the total cost of IGCT-SM is lowest due to the main switches with lower cost.

Complexity comparison of different protection solutions is illustrated in Table V. In the protection solution based on CP-IGCT and HS-FRD, CP-IGCT is compatible with the traditional mechanical and controlling parts. As a result, there is almost no change when using the protection solution. In the protection solution based on the IGBT with the active-clamp circuit, extra gate drive parts need to be arranged in the controlling board. And this will increase the complexity of the system. As for the protection solution based on the protection thyristor, it needs extra mechanical parts and gate drive besides the thyristor itself.

TABLE V
COMPLEXITY COMPARISON OF DIFFERENT PROTECTION SOLUTIONS BASED ON CP-IGCT, IGBT WITH ACTIVE-CLAMP CIRCUIT, AND PROTECTION THYRISTOR

Scheme	CP-IGCT	IGBT with active clamp circuit	Protection thyristor
Extra device	No	No	Yes
Extra gate drive parts	No	Yes	Yes
Extra mechanical parts	No	No	Yes
Total complexity	Lowest	Medium	Highest

Consequently, this protection solution is most complex compared with other two protection solutions.

VII. CONCLUSION

This article gives comprehensive analysis and experiment of extreme faults in the MMC based on the IGCT. A new protection solution based on CP-IGCT and HS-FRD is proposed for overcoming the extreme faults in the MMC system, which can replace the protection thyristor totally. Theoretical calculation shows that the proposed protection solution can help reduce the maximum fault current below 50% when the anode inductor is 0.8 μH in the extreme shoot-through fault. System-level experiment validation of the protection solution is carried out in an MMC system composed with 12 MMC-SMs. The surge current capability of HS-FRD is validated successfully in the dc pole-to-pole short-circuit fault test. And test results of the extreme shoot-through fault show that the proposed protection solution can realize discharge of the dc capacitor below 4.5 kV.

The maximum fault current in the MMC based on the IGCT is only about 600 kA. While the maximum fault current in the MMC based on the IGBT is over 1100 kA. Besides, the explosion proof of CP-IGCT is validated during the fault test, which is similar to that of the protection thyristor. However, IGBT cannot guarantee the package stability and may cause severe safety problem. SCFM of the failed CP-IGCT has also been validated and it can be used for bypass of the faulty MMC-SMs. Detailed

comparison among different protection solutions shows that the protection solution based on CP-IGCT and HS-FRD has lowest cost and complexity, as well as the highest safety.

REFERENCES

[1] H. Pang and X. Wei, "Research on key technology and equipment for Zhangbei 500kV dc grid," in *Proc. 8th Int. Power Electron. Conf.*, 2018, pp. 2343–2351.

[2] H. Rao et al., "Design aspects of the hybrid HVDC system," *CSEE J. Power Energy Syst.*, vol. 7, no. 3, pp. 644–653, May 2021.

[3] S. Gekenidis, E. Ramezani, and H. Zeller, "Explosion tests on IGBT high voltage modules," in *Proc. 11th Int. Symp. Power Semicond. Devices ICs*, 1999, pp. 129–132.

[4] O. Hohlfeld, "Damage protection of power modules," in *Proc. 9th Int. Conf. Integr. Power Electron. Syst.*, 2016, pp. 1–4.

[5] T. Wikström, B. Ødegård, and R. Baumann, "An 8.5 kV sacrificial bypass thyristor with unprecedented rupture resilience," in *Proc. 31st Int. Symp. Power Semicond. Devices ICs*, 2019, pp. 491–494.

[6] X. Zhang, G. Cao, and W. Zeng, "Research on application technology of sacrificial bypass thyristor suitable for VSC-HVDC system," in *Proc. 4th Int. Conf. HVDC*, 2020, pp. 26–30.

[7] H. Chen, F. Wakeman, J. Pitman, and G. Li, "Design, analysis, and testing of PP-IGBT-based sub-module stack for the MMC VSC HVDC with 3000A dc bus current," *J. Eng.*, vol. 2019, no. 16, pp. 917–923, Mar. 2019.

[8] S. Gunturi and D. Schneider, "On the operation of a press pack IGBT module under short circuit conditions," *IEEE Trans. Adv. Packag.*, vol. 29, no. 3, pp. 433–440, Aug. 2006.

[9] F. Wakeman, J. Pitman, and S. Steinhoff, "Long term short-circuit stability in press-pack IGBTs," in *Proc. 18th Eur. Conf. Power Electron. Appl.*, 2016, pp. 1–10.

[10] Z. Wang et al., "Research on the current flow mechanism of press-pack IGBT under short circuit condition in VSC-HVDC system," in *Proc. 4th Int. Conf. HVDC*, 2020, pp. 906–910.

[11] W. Zhou et al., "Current oscillation phenomenon of MMC based on IGCT and fast recovery diode with high surge current capability for HVDC application," *IEEE Trans. Power Electron.*, vol. 36, no. 6, pp. 6218–6222, Jun. 2021.

[12] P. K. Steimer, D. Weiss, and B. Odegard, "Robust, low-loss RCIGCT technology and MV applications," in *Proc. 10th Int. Conf. Power Electron.*, 2019, pp. 1703–1708.

[13] M. Buschendorf, J. Weber, and S. Bernet, "Comparison of IGCT and IGBT for the use in the modular multilevel converter for HVDC applications," in *Proc. 9th Int. Multi-Conf. Syst., Signals Devices*, 2012, pp. 1–6.

[14] S. Bernet, R. Teichmann, A. Zuckerberger, and P. K. Steimer, "Comparison of high-power IGBT's and hard-driven GTO's for high-power inverters," *IEEE Trans. Ind. Appl.*, vol. 35, no. 2, pp. 487–495, Mar./Apr. 1999.

[15] P. Ladoux, N. Serbia, and E. I. Carroll, "On the potential of IGCTs in HVDC," *IEEE J. Emerg. Sel. Topics Power Electron.*, vol. 3, no. 3, pp. 780–793, Sep. 2015.

[16] J. Liu et al., "A novel controlled punch-through IGCT for modular multilevel converter with over voltage bypass function," *IEEE Trans. Power Electron.*, vol. 36, no. 7, pp. 8280–8290, Jul. 2021.

[17] B. Zhao et al., "A more prospective look at IGCT: Uncovering a promising choice for dc grids," *IEEE Ind. Electron. Mag.*, vol. 12, no. 3, pp. 6–18, Sep. 2018.

[18] R. Zeng et al., "Integrated gate commutated thyristor-based modular multilevel converters: A promising solution for high-voltage dc applications," *IEEE Ind. Electron. Mag.*, vol. 13, no. 2, pp. 4–16, Jun. 2019.

[19] B. Ødegård, D. Weiss, T. Wikström, and R. Baumann, "Rugged MMC converter cell for high power applications," in *Proc. 18th Eur. Conf. Power Electron. Appl.*, 2016, pp. 1–10.

[20] D. Weiss, M. Vasiladiotis, C. Banceanu, N. Drack, B. Odegard, and A. Grondona, "IGCT based modular multilevel converter for an ac–ac rail power supply," in *Proc. Int. Exhib. Conf. for Power Electron., Intell. Motion, Renewable Energy Energy Manage.*, 2017, pp. 1–8.

[21] W. Zhou et al., "Comprehensive analysis, design and experiment of shoot-through faults in MMC based on IGCT for VSC-HVDC," *IEEE Trans. Power Electron.*, vol. 36, no. 6, pp. 6241–6250, Jun. 2021.

[22] M. Bruckmann, R. Sommer, M. Fasching, and J. Sigg, "Series connection of high voltage IGBT modules," in *Proc. IEEE Ind. Appl. Conf.*, 1998, pp. 1067–1072.

[23] J. Saiz, M. Mermet, D. Frey, P. O. Jeannin, J. L. Schanen, and P. Muszicki, "Optimisation and integration of an active clamp circuit for IGBT series association," in *Proc. Annu. Meeting Ind. Appl. Soc.*, 2001, pp. 1046–1051.

[24] T. Lu, Z. Zhao, S. Ji, H. Yu, and L. Yuan, "Active clamp circuit with status feedback for series-connected HV-IGBTs," *IEEE Trans. Ind. Appl.*, vol. 50, no. 5, pp. 3579–3590, Sep. 2014.

[25] S. Ji, T. Lu, Z. Zhao, H. Yu, and L. Yuan, "Series-connected HV-IGBTs using active voltage balancing control with status feedback circuit," *IEEE Trans. Power Electron.*, vol. 30, no. 8, pp. 4165–4174, Aug. 2015.

[26] F. Zhang, X. Yang, Y. Ren, L. Feng, W. Chen, and Y. Pei, "Advanced active gate drive for switching performance improvement and overvoltage protection of high-power IGBTs," *IEEE Trans. Power Electron.*, vol. 33, no. 5, pp. 3802–3815, May 2018.

[27] M. Beninger-Bina, T. Basler, M. Dainese, and H. J. Schulze, "A high-voltage transients suppressor diode," in *Proc. Int. Symp. Power Semicond. Devices ICs*, 2020, pp. 58–61.

[28] Infineon, *D4600U Datasheet, Fast Hard Drive Diode*. Neubiberg, Germany: Infineon, 2017.

[29] TOSHIBA, *ST3000GXH31A Datasheet, Press Pack IEGT*. Tokyo, Japan: Toshiba, 2020.

[30] ABB, *5SHY55L4500 Datasheet, Asymmetric Integrated Gate Commutated Thyristor*. Zürich, Switzerland: ABB, 2013.

[31] K. Jacobs, S. Norrga, and H. Nee, "Dissipation loop for shoot-through faults in HVDC converter cells," in *Proc. Int. Power Electron. Conf.*, 2018, pp. 3292–3298.

[32] W. Zhou et al., "Systematic analysis and characterization of extreme failure for IGCT in MMC-HVDC system—Part I: Device structure, explosion characteristics, and optimization," *IEEE Trans. Power Electron.*, vol. 37, no. 7, pp. 8076–8086, Jul. 2022.

[33] W. Zhou et al., "Systematic analysis and characterization of extreme failure for IGCT in MMC-HVDC system—Part II: Failure mechanism and short circuit characteristics," *IEEE Trans. Power Electron.*, vol. 37, no. 5, pp. 5562–5573, May 2022.

Wenpeng Zhou (Member, IEEE) was born in Heilongjiang, China, in 1995. He received the B.S. and Ph.D. degrees in electrical engineering from the Department of Electrical Engineering, Tsinghua University, Beijing, China, in 2017 and 2022, respectively.

He is currently a Postdoctoral Fellow with the Department of Electrical and Computer Engineering, The Hong Kong University of Science and Technology, Hong Kong. His current research interests include modeling and development of ultrawide-bandgap semiconductor devices, and optimization and application of the high-power integrated gate commutated thyristor for the HVdc system.

Biao Zhao (Senior Member, IEEE) was born in Hubei, China, in 1987. He received the B.S. degree in electrical engineering from the Department of Electrical Engineering, Dalian University of Technology, Dalian, China, in 2009, and the Ph.D. degree in electrical engineering from the Department of Electrical Engineering, Tsinghua University, Beijing, China, in 2014.

He is currently an Associate Professor with the Department of Electrical Engineering, Tsinghua University. His current research interests include high power converter, high power semiconductor device, and flexible dc transmission and distribution system.

Dr. Zhao is a Senior Member of the Chinese Society for Electrical Engineering and the Chinese Electro-technical Society.

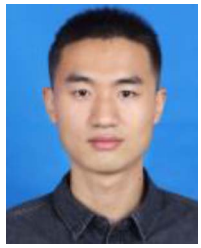

Ruihang Bai (Student Member, IEEE) was born in Shaanxi, China, in 1998. He received the B.S. degree in electrical engineering from the Department of Electrical Engineering, Tsinghua University, Beijing, China, in 2020, where he is currently working toward the Ph.D. degree in electrical engineering.

His current research interests include power electronic transformers and flexible dc transmission and distribution systems.

Yantao Lou was born in Henan, China, in 1982. He received the B.Sc. and M.Sc. degrees in electrical engineering from the Department of Electrical Engineering, Tsinghua University, Beijing, China, in 2006 and 2018, respectively.

He is the Deputy General Manager with Xi'an XD Power Systems Co., Ltd, Xi'an, China, in charge of the company's technology and R&D work. He is currently working in complete design of HVdc transmission system and the development of converter valve equipment.

Xiaoping Sun was born in Shaanxi, China, in 1985. She received the B.Sc. and M.Sc. degrees in electrical engineering from the School of Electrical and Control Engineering, Shaanxi University of Science and Technology, Shaanxi, in 2007 and 2010, respectively.

She is the Deputy Director with the DC Technology Department, Xi'an XD Power Systems Co., Ltd, Xi'an, China, and the Member of the Power Electronic Technology Subcommittee (SAC/TC60/SC2) of the National Power Electronic System and Equipment Standardization Technical Committee. She is currently involved in the research and development and engineering application of fully controlled power electronic products in the field of power transmission and distribution system.

Qi Liu was born in Shaanxi, China, in 1983. He received the B.Sc. and M.Sc. degrees in radio physics from the School of Physics and Optoelectronic Engineering, Xidian University, Shaanxi, in 2006 and 2009, respectively, and the Ph.D. degree in electrical engineering from the School of Electrical Engineering, Xi'an Jiaotong University, Shaanxi, in 2015.

He is the Director of the Electrical Room, DC Technology Department, Xi'an XD Power Systems Co., Ltd, Xi'an, China. He is currently involved in the research of HVdc thyristor converter valves and modular multilevel converter valves.

Jiapeng Liu (Student Member, IEEE) was born in Liaoning, China, in 1994. He received the B.S. and Ph.D. degrees from the Department of Electrical Engineering, Tsinghua University, Beijing, China, in 2016 and 2021, respectively.

He is currently a Postdoctoral Researcher with Tsinghua University. His current research interests include high power semiconductor device development and modeling.

Zhengyu Chen was born in Tianjin, China, in 1992. He received the B.S. and Ph.D. degrees in electrical engineering from Tsinghua University, Beijing, China, in 2014 and 2019, respectively.

After Ph.D., he became a Joint Postdoctoral Researcher with Tsinghua University and the University of Macau, Macau, China, in 2019. He is currently working with DC Research Center, Energy Internet Research Institute, Tsinghua University. His current research interests include power semiconductor devices and their gate unit drivers, HVdc systems, and dc circuit breakers.

Jinpeng Wu was born in Hebei, China, in 1987. He received the B.S. and Ph.D. degrees in electrical engineering from the Department of Electrical Engineering, Tsinghua University, Beijing, China, in 2010 and 2015, respectively.

From 2016 to 2020, he continued his research with Stanford University and Lawrence Berkeley National Lab as a Postdoctoral Researcher. He is currently working as an Associate Professor with the Department of Electrical Engineering, Tsinghua University. His research interests include the energy and electrical materials, power electronics, and X-ray spectroscopies.

Zhanqing Yu (Member, IEEE) was born in Inner Mongolia, China, in 1981. He received the B.Sc. and Ph.D. degrees in electrical engineering from the Department of Electrical Engineering, Tsinghua University, Beijing, China, in July 2003 and July 2008, respectively.

After graduation, he became a Postdoctoral Fellow and Lecturer with the Department of Electrical Engineering, Tsinghua University, in July 2008 and July 2010, respectively, where he became an Associate Professor in December 2012. His research interests include dc grid, dc breaker, electromagnetic environment, electromagnetic compatibility, and lightning protection.

Dr. **Yu** has participated in several projects sponsored by High-Tech R&D Program (863 Program), National Basic Research Program of China (973 Program), and the National Natural Science Foundation of China.

Rong Zeng (Senior Member, IEEE) was born in Shaanxi, China, in 1971. He received the B.Eng., M.Eng., and Ph.D. degrees in electrical engineering from the Department of Electrical Engineering, Tsinghua University, Beijing, China, in 1995, 1997, and 1999, respectively.

He was a Lecturer with the Department of Electrical Engineering, Tsinghua University, in 1999, where he was also an Associate Professor and a Professor in 2002 and 2007, respectively. He is currently working in the fields of air gap discharge, lightning protection, and electromagnetic compatibility in power systems, electric and magnetic field measurement by integrated electro-optical sensors, power semiconductor, HVdc system, and dc circuit breaker.